Title: Assessment of simple adhesive substrates as a method for quantifying microplastics and the factors influencing capture

Authors: Julie M. Rieland[^], Zeyuan Hu[&], Julian S. Deese[&], and Brian J Love[^&#]
The University of Michigan
[&]Department of Materials Science and Engineering
[#]Department of Biomedical Engineering
[^]Macromolecular Science and Engineering Graduate Program

2300 Hayward St
Ann Arbor, MI 48109

Corresponding author: BJ Love, bjlove@umich.edu, 734-763-2013

Highlights:
1.) Microplastic quantification strategies require greater standardization and better understanding of methodology bias
2.) An optical method for gauging microplastic adsorption has been developed
3.) Higher capture rates correlate with both microplastics concentration and binding time
4.) Schemes to consider competitive binding of particulate mixtures are presented

Keywords: adhesives; separation; microplastics; imaging; aggregate; dispersion

Abstract

Microplastics are a growing environmental concern, with a large body of evidence documenting distribution of plastic material in virtually all environmental compartments. Countermeasures that help to bind, aggregate, or coalesce these collections might result in lower human and animal exposures. Pressure sensitive adhesives (PSAs) have been identified as a viable microplastic (MP) capture mechanism with a range of potential use conditions. As with any countermeasure, there is a need to evaluate potential solutions in terms of collection efficiency, cost, ease of installation, robustness etc. Expanding on our previous work, spray-coated PSAs were investigated as submerged surfaces for use in a quick and low-cost quantitative method to assess MP binding in aqueous mediums. Resins containing two differing molecular weights of poly(2-ethylhexyl acrylate) PSA (92k and 950k), and a 50:50 by weight mixture of the two resins were applied as spray-coated substrates to compare the effect of resin composition on MP-adhesive binding. Thin films of PSA (92k 6 ± 1 μm, 950k 4 ± 2 μm, 50:50 BD 6.5 ± 1 μm) were sprayed on borosilicate glass slides using a commercial air brush. Polydisperse nylon-12 particles varying in size from 15-30 μm in diameter were dispersed in water at concentrations between 0.01 and 5 mg mL^{-1} and agitated under ambient conditions to assess adhesive binding as quantitative comparisons of microparticle capture. Mixed assays were also performed comparing binding of common MP species including polyethylene (50, 200 μm), polystyrene (10 μm), and polyester fibers (1000 μm) to understand how varying composition, size, and form factor affect adsorption. The glass slide method showed increasing linear trends of particle binding with increased

adhesive exposure time and MP concentration. The adhesive wettability to particles demonstrates bounding parameters under which softer adhesives excel at MP capture but may compromise adhesive film integrity. Low cost, ease of sample preparation, and small footprint of the adhesive testing method suggest promise for research use in under-resourced regions and field work.

1. Introduction

Since the 1950s, annual global plastic production has increased from 1.7 to 348 million tons in 2017 linked with increasing demand[1,2]. Furthermore, a 2018 energy report forecasted a 20% increase in petrochemical capacity (including plastics, lubricants, and organic solvents) as a share of oil and gas consumption growth over the next 20 years[3]. Despite this increasing rate of plastic consumption and production, understanding of how plastic waste accumulation affects global health and development of corresponding remedial solutions continue to lag[4]. Due to the high chemical stability of plastics, natural removal of plastic debris from the environment is limited[5]. Instead, plastic debris tends to fractionate by several mechanisms (UV, mechanical damage, abrasion) with increasing environmental exposure, where meso and micro fragments accumulate[5]. Microplastics (MPs) are generally defined as plastics with the largest dimension being less than 5mm and greater than 100 nm[6].

MPs have been identified as a growing problem, and with more awareness comes the need for both diverse and more targeted solutions[7,8]. Within the space of experimental and commercial MP remediation, most capture and removal is accomplished by physical filtration[9,10]. While reducing filter pore sizes results in broader, more effective MP capture, finer filters reduce filtration throughput and increase pressure drops across the filter, as commonly experienced with mask materials[11]. Furthermore, filters are only as effective as the ensuing waste management of the residual, which for filter residues of waste water treatment plants, is commonly redistributed back into the environment as fertilizer[5,12]. Recently, surface-chemistry based affinity and binding of MPs has gained interest. A variety of adsorption and isolation modes have been explored including π−π interactions[13], hydrophobicity[14,15] electrostatics[16–19], coagulation[20], and van der Waals forces[21,22]. Natural binding and adhesion in mussels and coral has also been identified as a potentially significant sink of ocean MPs[23,24] and has inspired new ideas[21].

Bench-scale, surface-chemistry based binding systems have proven effective in sterile environments devoid of impurities, with many surpassing 90% capture of MPs in pure water and water-ethanol solutions[13,16,17,22]. Binding via surface chemistry, however, tends to require long exposure times (> 30 minutes) to achieve the reported removal results. We've been considering faster binding modes using pressure sensitive adhesives (PSAs) deployed in water that rapidly achieve adequate removal efficiencies within ~5 minutes of exposure[22]. PSAs are adhesives that retain a soft, viscoelastic character, where bonding is initiated by applying pressure, and adherends can be removed without adhesive residue [25,26]. The adhesive mechanism largely depends on the viscoelastic behavior of the polymer with contributions from the thermodynamic driving force of surface energy interactions [25,27]. Since MPs exist in a diverse array of sizes, form factors, and compositions, there is a broader need to assess the binding affinity of particles on a given collision with the adhesive substrate, as well as the longevity of any given binding event.

Due to the general mechanical requirements of PSAs[28], there is also a concern regarding the integrity of adhesive coatings under surf zone turbulence and other shear force stimuli.

While preliminary assessments of PSA based systems are promising, there is a need to compare methods to gauge the robustness and limitations of any binding mechanism. We propose an observational protocol for an adhesive-coated substrate in exposure testing with microplastic dispersions to probe parametric binding with different adhesives, particles, and environmental conditions. Herein we present our methodology for preparing adhesive-coated substrates, experimental conditions, and the analysis procedures for observing MPs captured from aqueous dispersion. Adhesive binding is tested with several MPs both independently and in competitive assays demonstrating pathways to assess how MP composition, size, and shape affect binding. Schemes to gauge robustness and effectiveness of this system are also presented.

2. Method and Materials

2.1 Materials

Poly(2-ethylhexyl acrylate) (PEHA) in toluene solution reported as 92 kg mol^{-1} (92k) was purchased from Sigma Aldrich then subsequently dried on a rotary evaporator. Tetrahydrofuran (THF), Tergitol® 15-S-9, and methanol were purchased from Fisher Scientific. Materials for the synthesis of 950 kg mol^{-1} (950k) PEHA **(SI)** were used as received unless specified. Polyacrylic acid (PAA) reported as 1,033 kg mol^{-1} was purchased from Scientific Polymer Products. 2-ethylhexanol and sulfuric acid (H_2SO_4) were purchased from Millipore Sigma. Borosilicate glass slides (25 x 75 x 1mm) were purchased from Fisher Scientific. A variety of microplastics (MPs) were acquired and used as received unless specified otherwise. Nylon-12 powder (avg size ~30 µm) (Nylon30) was obtained from Goodfellow Cambridge Ltd. PE microspheres (#CPMS-0.96 45-53 µm, avg size ~50 µm) (PE50) and PS microspheres (#PSMS-1.07 9.5-11.5 um, avg size ~10 µm) (PS10) were obtained from Cospheric. Commercial PET yarn was purchased from Joann Fabrics and cut with a straight razor to ~1mm long fibers, cut yarn was subsequently processed in an electric coffee grinder to break up clumping. Post-Consumer PE was acquired as an empty vinegar bottle which was cryo-ground in a SPEX SamplePrep 6775 Freezer/Mill (avg size ~200 µm) (PE200). Silica sand was provided by the VanVlack Undergraduate Laboratory, and bentonite clay was purchased from Adventures in Home Brewing, Ann Arbor.

2.2 Methods

2.2.1 Coating glass slides

Glass slides were prepared by washing the designated adhesive zone with acetone. 92k PEHA at 5% w/v was dissolved at room temperature in tetrahydrofuran (THF) and dispensed from an AGPTEK Mini Airbrush (Amazon). The slides were coated using a circular brushing motion for 3 seconds while the airbrush is held at a distance of 10 cm from the slide. Slides were then stored in a ventilated box at room temperature for at least 24 hours to allow for solvent evaporation. 950k PEHA at 2% w/v was dissolved in THF in an airtight vial at 60°C in an oven and immediately airbrushed for 5 seconds onto cleaned glass slides. 50:50 bimodal distributions (50:50 BD) were produced on an equal weight basis of 92k and 950k PEHA. For 50:50 BD, 0.1 g of 92k and 0.1 g

of 950k were dissolved in 10 mL of THF at 60°C for a net 2% w/v polymer in solvent. Adhesive solutions were airbrushed immediately upon removal from the 60°C oven to leverage the lower resin viscosity at elevated temperature and improve airbrush flowrates. Adhesive deposition on glass slides was confirmed by both optical microscopy and SEM (JEOL JSM-IT500HR) imaging. The film thickness was measured by assessing the side profile of the glass slides under SEM identifying 92k films at 6 ± 1 µm, 950k at 4 ± 2 µm, and 50:50 BD at 6.5 ± 1 µm with relatively smooth surface finishes.

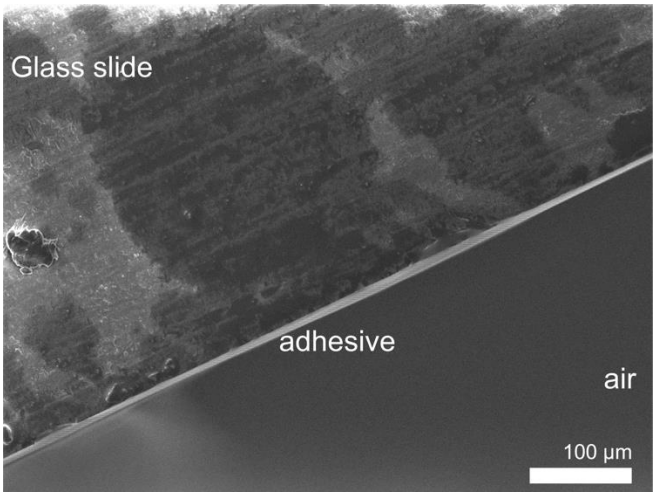

Figure 1. SEM micrograph demonstrating an edge-on view of the 92k Poly (2-ethylhexyl acrylate) coating on a glass slide.

2.2.2 Shake tests

Four testing protocols were assessed. First, calibration curves were generated by immersing adhesive-coated glass slides in nylon MP dispersions to demonstrate MP concentration and exposure time dependencies. DI water was mixed with nylon-12 particles with an average dimension of 30 µm (Nylon30) to form dispersions at 0.01, 0.1, 1, 2, and 5 mg mL^{-1}. Some instantaneous binding was noted on the adhesive as slides were immersed. Time-dependent binding was studied at 1, 5, 10, and 30-minute trials for 1 mg mL^{-1} Nylon30 with 950k and 50:50 BD PEHA. Next, the influence of select soluble and insoluble interferents on nylon adsorption were tested using 92k, 950k, and 50:50 BD adhesives. Lastly, shake tests were also performed using 950k PEHA with other MP species. The MPs selected were 50 and 200 µm polyethylene (PE50, PE200), 10 µm polystyrene (PS10), and 1000 µm polyester fibers (PET1000). Individual species were tested at 0.1 mg mL^{-1} (PS10, PET fibers) as well as in mixed assays on an equal weight basis with each component MP dispersed at a concentration of 0.1 mg mL^{-1} (PS10/Nylon30, PE50/PE200, PS10/Nylon30/PET fiber). More details on methodology and interferant preparation is available in the **SI**.

Shake test samples at concentrations greater than 0.5 mg mL^{-1} were prepared in individual 30 mL volumes rather than general stock dispersions to reduce dispensing errors due to generally poor dispersion of particles. MPs and solid interferents were weighed out on an analytical scale and added to 50mL glass vials, followed by 30mL of DI water or interferant stock solutions measured

out in a graduated cylinder. After vigorously shaking sample vials by hand, the coated slides were deposited. For bentonite interferant tests, the nylon and bentonite were allowed to hydrate for 5 minutes before shake testing. Samples were then shaken on a Thermo Scientific multi-purpose rotator table at 200 RPM for the designated exposure time. Samples were run in triplicate at ambient temperature and secured to the rotator platform in a padded and weighted cardboard box. After shaking, glass slides were removed from the vials and rinsed on both sides with DI water (20mL) to remove particles weakly or not bound by the adhesive. Slides were then dried overnight, covered by 3-inch petri dishes to prevent errant dust collection. Mixed assays were performed using deliberately low concentrations to minimize aggregation and overlapping on the adhesive surface for imaging. Data on PET yarn binding can be found in the **SI**.

2.2.3 Observational assessment

Briefly, adhesive regions on dried glass slides were imaged on a Nikon Eclipse LV100ND microscope with a DS-RI2 camera before and after exposure to MP dispersions. Each slide was imaged 3 times in a pre-assigned diagonal pattern across the adhesive region to control for bias. The imaging location was adjusted slightly in the case of large defects in the adhesive or the rare presence of contamination (e.g., unexpected fibers). Image processing was performed in the ImageJ® software to collect number count and planar surface area (SA) for particles and particle clusters in each image. Objects with a planar surface area less than 85 μm^2 were omitted as dust and other extraneous discoloration. The values determined from the 3 images were then aggregated for each slide to determine an average surface area coverage (%SAC) as calculated with equation 1. More in-depth description is available in the **SI**.

$$\%SAC = ((\sum SA_{particles\ and\ clusters}) / (3*SA_{image\ area})) \times 100 \qquad \text{Eqn 1}$$

3. Results and Discussion

The binding affinity of aqueous-dispersed Nylon particles with poly(2-ethylhexyl acrylate) (PEHA) adhesives was compared for a range of MP concentrations, times, and interferants. Microscope images were processed with ImageJ software to yield particle count and SA measurements to calculate net percent surface area coverage (%SAC) as a gauge of binding affinity. Nylon was selected for its wide availability and its higher dispersion capacity compared to PE and PP, which are more common, but are both more buoyant and hydrophobic. As a model study we used DI water as a controlled variable to facilitate assessment of different adhesive formulations, environmental conditions, and plastic compositions. The overriding goal was to assess the potential of the adhesive binding without complicating factors relating to water hardness, pH, and other dissolved solids.

To make differences in binding more visible, we assessed binding primarily at elevated concentrations (1–5 mg mL^{-1}) compared to most aqueous environmental concentrations, which are highly dependent on time and location[29]. To test for transferability to more dilute conditions we also assessed binding at 0.01 mg mL^{-1} nylon30 with 2 of our 3 adhesives. After 5 min of shaking, the 950k had 0.13 ± 0.1 % surface area coverage (SAC). The experiment was repeated

using a mixed, bimodal distribution of 50% 92K and 50% 950K (50:50 BD) and shaken for 30 mins yielding 0.27 ± 0.1 % SAC, showing that binding is measurable at 0.01 mg mL^{-1} and that adhesive formulation and increased time can improve capture.

The binding distribution of MPs varied across the surface of the adhesive, with higher binding around the periphery of each spray-coated adhesive region and reduced binding in the center (**SI**). A regimented imaging protocol analyzed 3 images taken in a diagonal pattern across the adhesive region to control for heterogenous adsorption. All samples demonstrate relatively high variance, which could be caused by a variety of factors including nylon30's higher density relative to water, static interactions with the walls of the test vessels, as well as particle aggregation along the edges of the glass slide. Previously, adding ethanol to aqueous solutions has been reported to improve dispersion quality of MPs by reducing aqueous surface tension[18,22]. However, changing the composition of the fluid medium by adding ethanol changes the fluid density, adhesion energetics of the system, and also plasticizes the adhesive. We assessed the influence of 3 concentrations of ethanol (20%, 40%, and 60%) in DI water on MP capture and identified moderate reductions in variance **(SI)**. However, we opted for DI water to more closely represent an objective study.

3.1 Resin variations: impact on binding

Figure 2 shows select images of the adhesive surfaces with nylon30 binding incidence. Comparison of the MP binding behavior between the two different molecular weight adhesives and the resin mixture demonstrates faster binding for the 92k PEHA compared to 950k at all time points. However, when particle exposure times were longer than 1 minute, the 92k resin migrated on the slide surface and coalesced around dense aggregations of particles. Although the capture with the 92k resin is effective, as demonstrated by the dense packing of particles observed at 5 and 10 minutes **(Figure 2)**, the loss of a cohesive film made image-based counting inconclusive. The high mobility of the adhesive could also lead to shedding, which may account for unidentified small particles observed in our previous work[22]. The 950k resin deposited on slides also shows binding, with more stable films persisting through 5 minutes of exposure time **(Figure 3)**. The general lower binding of the 950K resin is attributed to a higher adhesive modulus, as measured through rheology**(SI)**, which may lead to less binding after particle collision[25]. Higher stiffness could also result in a "catch and release" scheme where captured particles are temporarily bound [30]. Interestingly, the 50:50 BD had higher binding affinity and more robust film stability due to plasticization of the 950k by the 92k resin. 50:50 BD films were generally stable through 30 minutes of aqueous exposure, although some film deterioration was noted. In the literature, bimodal resin distributions have been shown to improve bulk polymer properties such as flow, loop tack, and shear strength in both PSAs[31] and elastomers[32]. The results are instructive, but further exploration into adhesive formulation and compounding is needed to optimize capture.

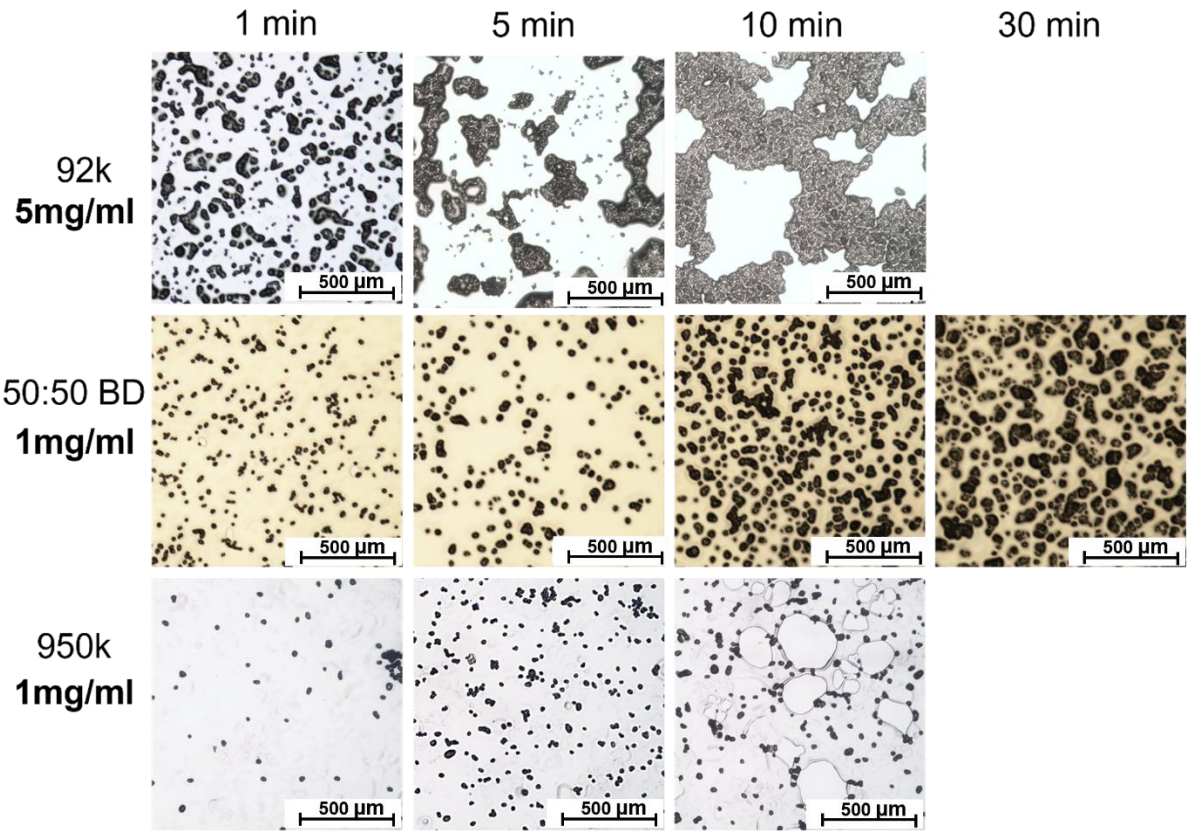

Figure 2. Time based capture of nylon30 from DI water on adhesive-coated glass slides. 92k tests were performed with 5 mg mL^{-1} of nylon30. 950k and the 50:50 bimodal distribution (BD) tests were performed with 1 mg mL^{-1} nylon30. In the 92k sample at the 5 and 10 minute marks, cavities represent the absence of adhesive due to adhesive migration and coalescence. The 950k at 10 minutes also shows some adhesive migration.

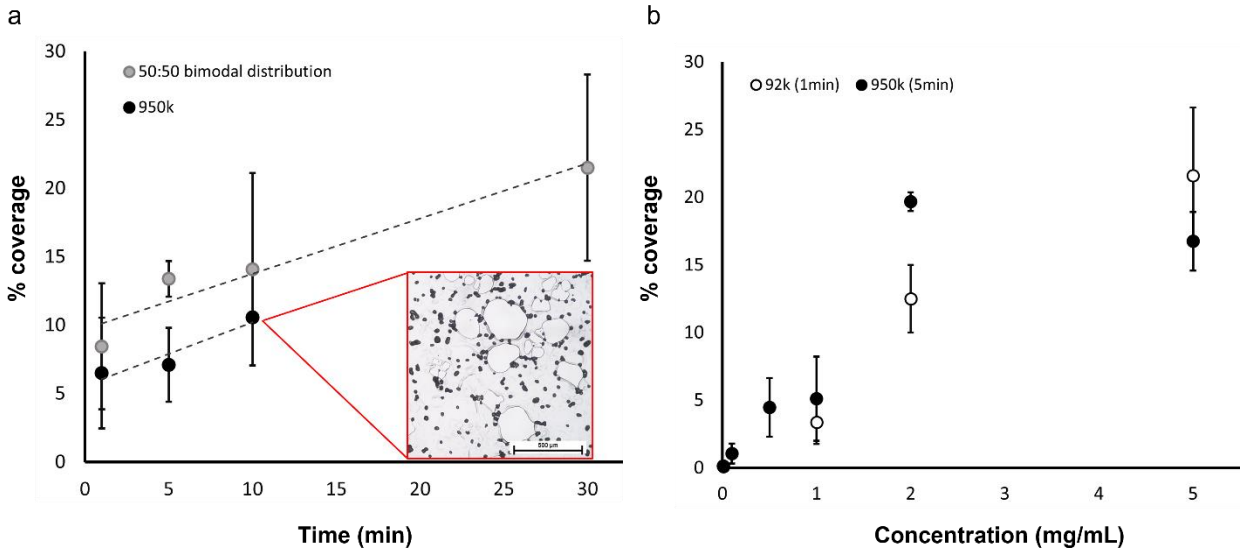

Figure 3. a) Plot of time-based assessment versus %SAC for 950k and 50:50 BD of PEHA each with 1 mg mL^{-1} of nylon30 from DI water. b) Plot of %SAC versus concentration of nylon30 for 950k at 5 min shaking and 92k at 1 min shaking in DI water

Glass slide aggregate data shows increasing trends in microplastic binding with both MP concentration and exposure time **(Figure 3a,b)**. Although not statistically significant, **Figure 3a** shows a positive linear trend between MP capture and time, and there is evidence that adhesive formulation can substantially shift binding affinity. Time-dependent capture was also impacted by film stability as the 950k adhesive degraded after 10 minutes of exposure, and the 92k was unable to be assessed after 1 minute due to resin migration **(Figure 2)**. This was also highlighted by the similar performance of the 950k at 5 min shaking and the 92k at 1 min shaking.

3.2 Impact of interferents and more realistic dispersions found in the built environment

Adhesive binding of nylon30 particles was assessed when dispersed in tap water, 35% saline solution, samples of water taken from the Huron River, and aqueous dispersions of surfactants (ionic and non-ionic), humic acid, silica sand, bentonite clay, and DI water samples cooled to 3°C (**Figure 4**). Binding data is presented in **Table 1**. The microplastic capture was reduced compared to the DI water controls under all conditions except for the 1mg mL^{-1} silica sand which performed 3% better than the control. Binding in hard tap water and water sampled from the Huron River was also within one standard deviation of the control, however the variance was larger for these tests. Overall, adhesive binding was found to be viable under all conditions tested although the adsorption was severely disrupted by non-ionic surfactants (Tergitol, **4f**), 3° C DI water **(4b)**, and bentonite clay **(4l)**. Several interferants also degraded the adhesive including SDS ionic surfactant **(4d)**, humic acid **(4e)**, and silica sand **(4k)**, which negatively impacted quantification. The interaction between the environment and the adhesive is the greatest barrier to developing more robust films. In **Figure 4**, all 3 adhesive formulations (92k, 950k, and 50:50 BD) are represented as a result of progressive improvements in understanding of adhesive properties, however they are all composed of the same PEHA functional units and expected to have similar surface energetics.

Table 1. Surface area coverage of nylon30 particles under different environmental interferants

Adhesive	Nylon30 Conc.	Shake time	Interferant^	%SAC
92k PEHA	5 mg mL^{-1}	1 min	DI water	21.6 ± 5.0
			3° C DI water	12 ± 5.2
			35% Saline	11 ± 2.3
			SDS 0.1% w/v	*
			Humic acid 200 mg/L	*
			Tergitol 0.1% w/v	1.0 ± 0.5
950k PEHA	5 mg mL^{-1}	1 min	DI water	19.0 ± 5.8
			Huron River water	15.9 ± 7.4
			Tap water	13.3 ± 6.7
50:50 BD	1 mg mL^{-1}	5 min	DI water	13.4 ± 1.3
			Silica sand 1 mg mL^{-1}	13.8 ± 1.8
			Bentonite clay 1 mg mL^{-1}	2.0 ± 0.8

^*All samples are prepared in DI water except Huron River water and Tap water*

These interferents degraded the adhesive too much to assess %SAC

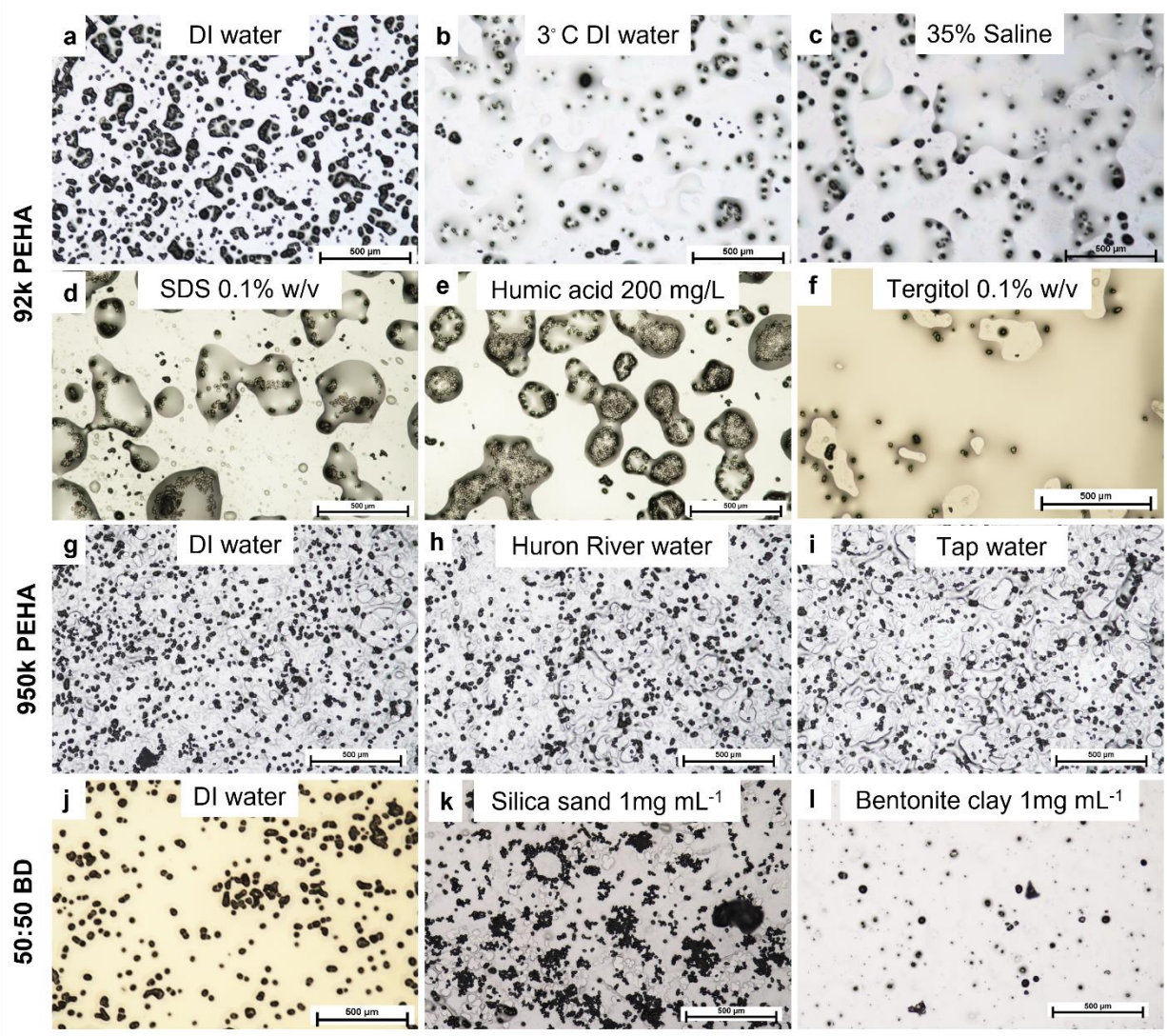

Figure 4. Optical microscope images showing nylon adsorption in the presence of varying environmental interferants. Results for 5 mg mL^{-1} of nylon and 1 minute of shaking are shown for 92k PEHA (a-f) and 950k PEHA (g-i). Results for 1 mg mL^{-1} of nylon and 5 minutes of shaking with a 50:50 bimodal distribution are depicted in (j-l).

The 92k was the softest and most unstable of the 3 formulations tested, and it was substantially compromised by the SDS **(4d)** and humic acid **(4e)**, which appear to have plasticized the 92k, leaving islands of adhesive with embedded clusters of nylon particles. However, because it is so soft, the low glass transition temperature likely positions it to function better in low temperature conditions where it's tack would be higher than more glassy resins. The insoluble silica (100 µm) was also destructive to the adhesive. We did not see substantial adhesion of sand to the adhesive **(4k)**, but there was noticeable abrading of the 50:50 BD suggesting that the plasticized thermoplastic film is weak to collisions with higher density particles.

The Tergitol **(4f)** and bentonite **(4l)** are unique cases where the interferent fouls the adhesive surface. Preliminary computational assessment demonstrates that Tergitol binds to PEHA under aqueous conditions[33]. Likewise, the bentonite visibly fouls the adhesive surface with small particulate material. We are currently studying surface energy energetics under a range of aqueous interferents and will report on this in future publications.

3.3 Binding assessments using mixed particulates

In mixed assays, MPs were specifically selected to be distinct in size and/or shape to distinguish using built-in ImageJ features **(SI)**. Several representative images were used to calibrate the size range and circularity factor for individual particle types, and those conditions were applied to the rest of the images. When quantifying particles, aggregates of the same particle species were treated as larger individual particles for particle counting and surface area assessments. Individual images were excluded from the analysis when aggregation and/or overlap of different particle types was frequent and when aggregate formation of one species compromised size-based particle identification in ImageJ.

Combinations of common plastic species were assessed to study the influence of MP composition (PS10/nylon30) and particle size (PE50/PE200). Individual parametric studies were also performed for both PS10 and cut PET fibers at 0.1 mg mL^{-1} respectively which are included in the **SI**. Adsorption was assessed on both metrics of %SAC and number count. In the PS10/nylon30 test, the nylon30 particles adsorbed at similar rates as in pure nylon30 tests, while PS10 binding in mixed conditions was lower compared to pure PS10 tests. A 73% reduction in %SAC between pure PS10 tests and PS10/nylon30 mixed conditions was noted based on particle differentiation with ImageJ **(Figure 5)**. Figure 5c shows aggregates of PS10 that could be misidentified as larger nylon30 particles, which may have undercounted PS10 in the mixed assay. It's also possible that co-binding between the two particles occurs. The lower PS10 binding could be a result of the more polar nylon30 having greater affinity for PEHA when mixed with PS10[30]. The larger nylon30 particles may also block the access of smaller PS10 particles to the adhesive substrate or dislodge particles that are insufficiently adsorbed. Overall, mixed assay assessment of PS10/nylon30 looks promising for image based assessment to quantify co-binding. Limitations exist with image resolution/analysis that could be improved with integration of other analytical techniques like Fourier transform infrared spectroscopy (FTIR) or Raman microscopy.

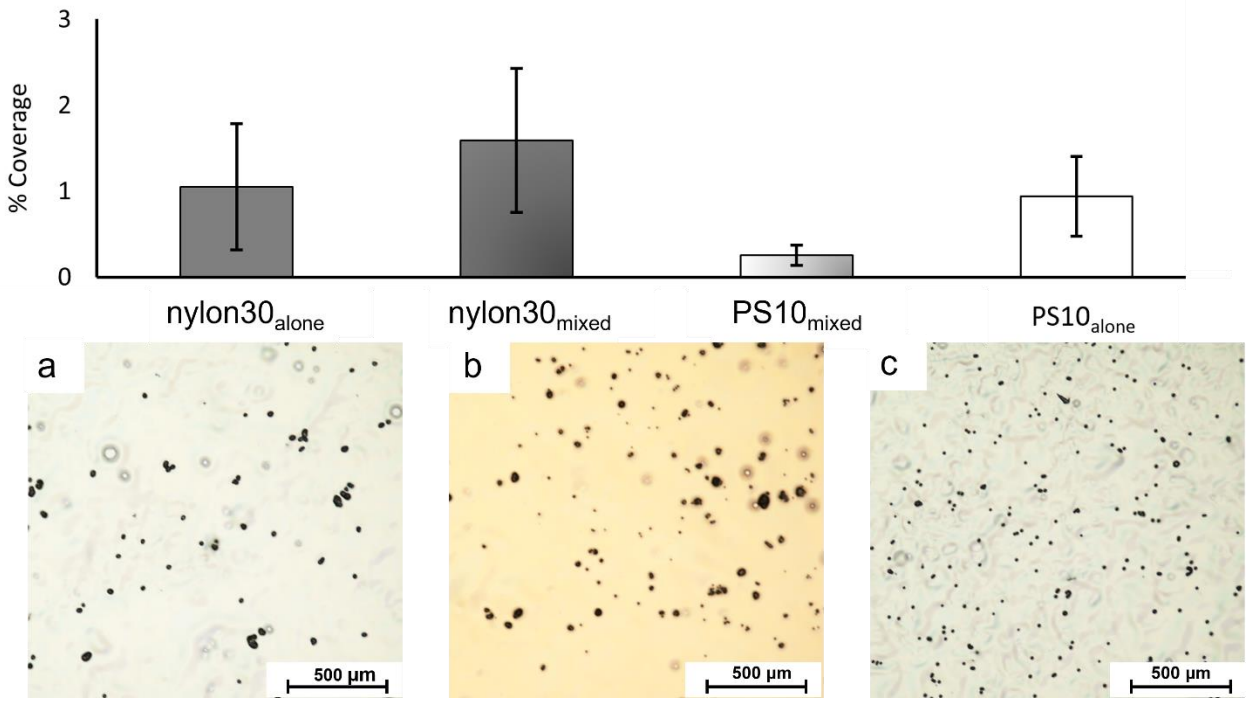

Figure 5. Comparison of %SAC for nylon30 and PS10 on 950k PEHA adhesive testing both parametrically and in mixed assay. A) 0.1 mg mL^{-1} nylon30 ($nylon30_{alone}$), b) mixed assay of 0.1 mg mL^{-1} of each nylon30/PS10 in DI water, c) 0.1 mg mL^{-1} PS10 ($PS10_{alone}$)

A second mixed assay was performed between polyolefin polymers PE50 and PE200 using the same 950K adhesive. These PE samples are much lower in density than nylon30 and are found near the meniscus of the aqueous fluid. The high buoyancy and hydrophobicity led to poor dispersion in water and relatively high levels of both homogenous and heterogenous aggregation in water and on adhesive surfaces **(SI)**. Heterogenous clusters in the images could not be deconvoluted using ImageJ software since ImageJ relies on grayscale pixel intensity and cannot differentiate discrete particle boundaries. More heterogenous aggregation was observed with the PE50/PE200 compared to the PS10/nylon30 mixtures, probably due to the shared composition and hydrophobicity of the two particle types. A comparison mixture with nylon30/PE50 wasn't possible due to size overlap of the polydisperse white powders. Consideration of more advanced visualization software is underway and will be presented in future work.

Comparing across polymer samples based on particle size and composition, the most significant binding trend was with particle size, where the type of measurement is shown to directly bias the interpretation of the data **(Figure 6)**. Regardless of the individual composition, the binding of smaller particles translated to more binding events per unit area and lower overall %SAC, whereas the binding of a few larger particles resulted in more coverage but lower incidence of binding. This exposes bias introduced by our decision to spike the solutions with mass-based concentrations, where a specified mass of smaller MPs inherently contains more particles than an equivalent mass of larger particles. The %SAC and count data presented in **Figure 6** were acquired simultaneously through ImageJ interpretation of the image sets, which is a strength of

the visual based assessment. Our findings could help bridge the literature gap between count based and mass based (comparable to %SAC) MP assessments[34,35]. Without knowing whether count or coverage is most telling, the reporting of only one mode of counting, especially in mixed particle systems can skew quantitative interpretations. To minimize bias and present the most accurate picture of MP presence, it seems best to present both values when sampling diverse MP distributions.

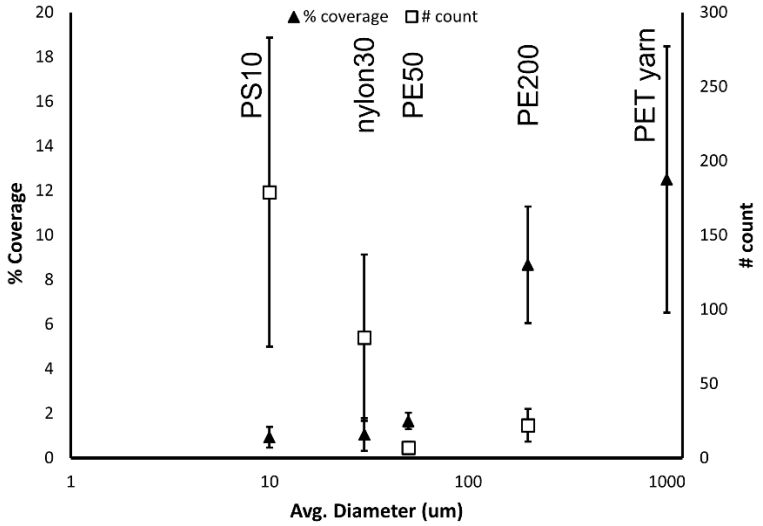

Figure 6 Plot of %SAC and particle count with respect to the particle average diameter for 0.1 mg/ml dispersions with 950k adhesive, 5 min shaking in DI water.

4. Conclusion

A simple, low-cost imaging-based assessment of MP capture was deployed using adhesive-coated glass slides to assess MP dispersions and to better understand adhesive-based capture. Three formulations of adhesives were tested with a selection of post-consumer and commercially available forms of MPs including nylon, PE, PET fibers, and PS. We developed an imaging protocol to analyze MP binding on adhesive-coated slides. Trends were established comparing capture efficiency with MP concentrations in aqueous solution and under a range of conditions altering particle types, particle concentration, adhesive exposure time, and a variety of soluble and in-soluble interferents.

As a comparative method, adhesive mediated MP binding is a simple and inexpensive tool that allows one to parameterize assessments based on adhesive, MP species, and other environmental conditions. The slide-based binding assessment can accommodate a wide range of particle sizes, both for analysis and as impurities, and is more granular than gravimetric techniques due to a higher sensitivity to small particles. The technique also permits the simultaneous collection of count and surface area data, while allowing for subsequent testing such as flow cytometry and hemocytometry if the particles are of appropriate size. The glass slide method also benefits from simplicity of analysis, that makes it accessible to researchers without access to expensive infrastructure like FTIR spectrometers, flow cytometers, scanning electron

microscopes (SEM), or even consistent access to internet. ImageJ is a self-contained image analysis tool that only has to be downloaded once, and then operates locally on the user's computer. Like other analysis tools, the slide observation technique has inherent limitations. The technique is affected by particle dispersion problems associated with polar interactions and density stratification, which contributes to heterogenous adhesive binding. The heterogenous binding adds to complications with the image-based assessment by compromising the current software's ability to identify discrete particles and fibers.

We also identified an inherent bias in MP quantification based on the units reported. In mixed MP collections as they commonly exist in the environment, weight-based assessments bias towards larger particles, and count based assessments bias towards smaller particles, both complicating the harmonization of data and muddying our ability to convey information to health professionals, policy makers, and the general public. Therefore, we propose reporting both number count and size-related (i.e. weight or surface area) data where possible to interpret MP collections objectively.

5. References

(1) PlasticsEurope. *Plastics – the Facts 2018: An Analysis of European Plastics Production, Demand and Waste Data*; 2018.

(2) Garcés-Ordóñez, O.; Castillo-Olaya, V. A.; Granados-Briceño, A. F.; Blandón García, L. M.; Espinosa Díaz, L. F. Marine Litter and Microplastic Pollution on Mangrove Soils of the Ciénaga Grande de Santa Marta, Colombian Caribbean. *Mar. Pollut. Bull.* **2019**, *145* (2), 455–462. https://doi.org/10.1016/j.marpolbul.2019.06.058.

(3) Taylor, M. $180bn Investment in Plastic Factories Feeds Global Packaging Binge. *The Guardian*. 2017.

(4) Prata, J. C.; da Costa, J. P.; Lopes, I.; Andrady, A. L.; Duarte, A. C.; Rocha-Santos, T. A One Health Perspective of the Impacts of Microplastics on Animal, Human and Environmental Health. *Sci. Total Environ.* **2021**, *777*. https://doi.org/10.1016/j.scitotenv.2021.146094.

(5) Duis, K.; Coors, A. Microplastics in the Aquatic and Terrestrial Environment: Sources (with a Specific Focus on Personal Care Products), Fate and Effects. *Environ. Sci. Eur.* **2016**, *28* (1), 1–25. https://doi.org/10.1186/s12302-015-0069-y.

(6) MSFD Technical Subgroup on Marine Litter. *Guidance on Monitoring Marine Litter*; 2013. https://doi.org/10.2788/99475.

(7) Yuan, Z.; Nag, R.; Cummins, E. Human Health Concerns Regarding Microplastics in the Aquatic Environment - From Marine to Food Systems. *Sci. Total Environ.* **2022**, *823*, 153730. https://doi.org/10.1016/j.scitotenv.2022.153730.

(8) Horton, A. A.; Walton, A.; Spurgeon, D. J.; Lahive, E.; Svendsen, C. Microplastics in Freshwater and Terrestrial Environments: Evaluating the Current Understanding to Identify the Knowledge Gaps and Future Research Priorities. *Sci. Total Environ.* **2017**, *586*, 127–141. https://doi.org/10.1016/j.scitotenv.2017.01.190.

(9) Conesa, J. A.; Ortuño, N. Reuse of Water Contaminated by Microplastics, the Effectiveness of Filtration Processes: A Review. *Energies* **2022**, *15* (7), 2432. https://doi.org/10.3390/en15072432.

(10) Ahmed, R.; Hamid, A. K.; Krebsbach, S. A.; He, J.; Wang, D. Critical Review of Microplastics Removal from the Environment. *Chemosphere* **2022**, *293* (January), 133557. https://doi.org/10.1016/j.chemosphere.2022.133557.

(11) Pourdeyhimi, B. Surgical Mask Particle Filtration Efficiency (PFE): The Standard Needs

to Be Updated. *J. Sci. Med.* **2020**, *2* (3), 1–11.
(12) Nizzetto, L.; Futter, M.; Langaas, S. Are Agricultural Soils Dumps for Microplastics of Urban Origin? *Environ. Sci. Technol.* **2016**, *50* (20), 10777–10779. https://doi.org/10.1021/acs.est.6b04140.
(13) Sun, C.; Wang, Z.; Chen, L.; Li, F. Fabrication of Robust and Compressive Chitin and Graphene Oxide Sponges for Removal of Microplastics with Different Functional Groups. *Chem. Eng. J.* **2020**, *393* (March), 124796. https://doi.org/10.1016/j.cej.2020.124796.
(14) Jiang, H.; Zhang, Y.; Bian, K.; Wang, C.; Xie, X.; Wang, H.; Zhao, H. Is It Possible to Efficiently and Sustainably Remove Microplastics from Sediments Using Froth Flotation ? *Chem. Eng. J.* **2022**, *448* (June), 137692. https://doi.org/10.1016/j.cej.2022.137692.
(15) Tang, Y.; Zhang, S.; Su, Y.; Wu, D.; Zhao, Y.; Xie, B. Removal of Microplastics from Aqueous Solutions by Magnetic Carbon Nanotubes. *Chem. Eng. J.* **2021**, *406* (August 2020), 126804. https://doi.org/10.1016/j.cej.2020.126804.
(16) Shen, M.; Hu, T.; Huang, W.; Song, B.; Zeng, G.; Zhang, Y. Removal of Microplastics from Wastewater with Aluminosilicate Filter Media and Their Surfactant-Modified Products: Performance, Mechanism and Utilization. *Chem. Eng. J.* **2021**, *421* (P1), 129918. https://doi.org/10.1016/j.cej.2021.129918.
(17) Batool, A.; Valiyaveettil, S. Surface Functionalized Cellulose Fibers – A Renewable Adsorbent for Removal of Plastic Nanoparticles from Water. *J. Hazard. Mater.* **2021**, *413* (November 2020), 125301. https://doi.org/10.1016/j.jhazmat.2021.125301.
(18) Chen, Y. J.; Chen, Y.; Miao, C.; Wang, Y. R.; Gao, G. K.; Yang, R. X.; Zhu, H. J.; Wang, J. H.; Li, S. L.; Lan, Y. Q. Metal-Organic Framework-Based Foams for Efficient Microplastics Removal. *J. Mater. Chem. A* **2020**, *8* (29), 14644–14652. https://doi.org/10.1039/d0ta04891g.
(19) Lee, M.; Choi, W.; Lim, G. Electrokinetic-Assisted Filtration for Fast and Highly Efficient Removal of Microplastics from Water. *Chem. Eng. J.* **2023**, *452*, 139152. https://doi.org/10.1016/j.cej.2022.139152.
(20) Lee, J.; Wang, J.; Oh, Y.; Jeong, S. Highly Efficient Microplastics Removal from Water Using In-Situ Ferrate Coagulation : Performance Evaluation by Micro-Fourier-Transformed Infrared Spectroscopy and Coagulation Mechanism. *Chem. Eng. J.* **2023**, *451* (P2), 138556. https://doi.org/10.1016/j.cej.2022.138556.
(21) Zhou, H.; Mayorga-Martinez, C. C.; Pumera, M. Microplastic Removal and Degradation by Mussel-Inspired Adhesive Magnetic/Enzymatic Microrobots. *Small Methods* **2021**, *5* (9), 1–9. https://doi.org/10.1002/smtd.202100230.
(22) Chazovachii, P. T.; Rieland, J. M.; Sheffey, V. V.; Jugovic, T. M. E.; Zimmerman, P. M.; Eniola-Adefeso, O.; Love, B. J.; McNeil, A. J. Using Adhesives to Capture Microplastics from Water. *ACS ES&T Eng.* **2021**, *1* (12), 1698–1704. https://doi.org/10.1021/acsestengg.1c00272.
(23) Huang, W.; Chen, M.; Song, B.; Deng, J.; Shen, M.; Chen, Q.; Zeng, G.; Liang, J. Microplastics in the Coral Reefs and Their Potential Impacts on Corals: A Mini-Review. *Sci. Total Environ.* **2021**, *762*, 143112. https://doi.org/10.1016/j.scitotenv.2020.143112.
(24) Li, J.; Wang, Z.; Rotchell, J. M.; Shen, X.; Li, Q.; Zhu, J. Where Are We? Towards an Understanding of the Selective Accumulation of Microplastics in Mussels. *Environ. Pollut.* **2021**, *286* (January), 117543. https://doi.org/10.1016/j.envpol.2021.117543.
(25) Li, L.; Tirrell, M.; Korba, G. A.; Pocius, A. V. Surface Energy and Adhesion Studies on Acrylic Pressure Sensitive Adhesives. *J. Adhes.* **2001**, *76*, 307–334. https://doi.org/10.1080/00218460108030724.
(26) Sun, S.; Li, M.; Liu, A. A Review on Mechanical Properties of Pressure Sensitive Adhesives. *Int. J. Adhes. Adhes.* **2013**, *41*, 98–106. https://doi.org/10.1016/j.ijadhadh.2012.10.011.
(27) Karnal, P.; Roberts, P.; Gryska, S.; King, C.; Barrios, C.; Frechette, J. Importance of

Substrate Functionality on the Adhesion and Debonding of a Pressure-Sensitive Adhesive under Water. **2017**. https://doi.org/10.1021/acsami.7b13984.
(28) Dahlquist, C. . Creep. In *Creep. Handbook of pressure sensitive adhesive technology*; Satas, D., Ed.; Satas & Associates: Warwick, 1999; pp 121–138.
(29) Li, W.; Li, X.; Tong, J.; Xiong, W.; Zhu, Z.; Gao, X.; Li, S.; Jia, M.; Yang, Z.; Liang, J. Effects of Environmental and Anthropogenic Factors on the Distribution and Abundance of Microplastics in Freshwater Ecosystems. *Sci. Total Environ.* **2023**, *856* (August 2022), 159030. https://doi.org/10.1016/j.scitotenv.2022.159030.
(30) Peykova, Y.; Lebedeva, O. V; Diethert, A.; Peter, M.; Willenbacher, N. Adhesive Properties of Acrylate Copolymers : Effect of the Nature of the Substrate and Copolymer Functionality. *Int. J. Adhes. Adhes.* **2012**, *34*, 107–116. https://doi.org/10.1016/j.ijadhadh.2011.12.001.
(31) Fonseca, G. E.; McKenna, T. F. L.; Dubé, M. A. Effect of Bimodality on the Adhesive Properties of Pressure Sensitive Adhesives: Role of Bimodal Particle Size and Molecular Weight Distributions. *Ind. Eng. Chem. Res.* **2010**, *49* (16), 7303–7312. https://doi.org/10.1021/ie100204x.
(32) Mark, J. E. Elastomeric Networks with Bimodal Chain-Length Distributions. *Acc. Chem. Res.* **1994**, *27* (9), 271–278. https://doi.org/10.1021/ar00045a003.
(33) Jugovic, T. M. E.; Zimmerman, P. M. *Private Communication*.
(34) Qiu, Q.; Tan, Z.; Wang, J.; Peng, J.; Li, M.; Zhan, Z. Extraction, Enumeration and Identification Methods for Monitoring Microplastics in the Environment. *Estuar. Coast. Shelf Sci.* **2016**, *176*, 102–109. https://doi.org/10.1016/j.ecss.2016.04.012.
(35) Mai, L.; Bao, L.-J.; Shi, L.; Wong, C. S.; Zeng, E. Y. A Review of Methods for Measuring Microplastics in Aquatic Environments. *Environ. Sci. Pollut. Res.* **2018**, *25* (1), 11319–11332.